Structural evolution of disordered $LiCo_{1/3}Fe_{1/3}Mn_{1/3}PO_4$ in lithium batteries uncovered

Ana Belen Muñoz Garcia,[a] Bernardino Tirri,[b] Isaac Capone,[c] Aleksandar Matic,[d] Michele Pavone[b,*] and Sergio Brutti[e,f,*]

[a] Dipartimento di Fisica "Ettore Pancini", Università di Napoli Federico II, Comp. Univ. Monte Sant'Angelo, Via Cintia, 21, 80126 Naples, Italy.

[b] Dipartimento di Scienze Chimiche, Università di Napoli Federico II, Comp. Univ. Monte Sant'Angelo, Via Cintia, 21, 80126 Naples, Italy.

[c] Department of Materials, University of Oxford, Parks Road Oxford OX1 3PH, UK.

[d] Department of Physics, Chalmers University of Technology, SE41296 Göteborg, Sweden

[e] Dipartimento di Chimica, Università di Roma La Sapienza, P.le Aldo Moro 5, 00185 Rome, Italy.

[f] ISC-CNR, UOS Sapienza, Via dei Taurini, 00185 Rome, Italy.

Supplementary material

Table S1. List of the *post mortem* samples studied by ex-situ synchrotron XRD

Samples recuperated at various stages of charge (oxidation)			
Sample label	State of charge	Nominal Li content (x) Li_xTMPO_4	Experimental Li content (y) Li_yTMPO_4
OCV	Pristine sample	1.00	1.02 ± 0.04
C15%	Charged for 6 h	0.85	0.86 ± 0.05
C33%	Charged for 13.2 h	0.67	0.69 ± 0.04
C36%	Charge for 14.4 h	0.64	0.67 ± 0.03
C50%	Charged for 20 h	0.50	0.53 ± 0.05
C67%	Charged for 26.8 h	0.33	0.39 ± 0.02
C70%	Charged for 28 h	0.30	0.38 ± 0.02
C80%	Charged for 32 h	0.20	0.27 ± 0.02
C90%	Charged for 36 h	0.10	0.18 ± 0.02
C100% or D0%	Charged for 40 h End of charge	0.00	0.09 ± 0.01
Samples recuperated at various stages of discharge (reduction)			
Sample label	State of discharge after a full charge of 40h	Nominal Li content (x) Li_xTMPO_4	Experimental Li content (y) Li_yTMPO_4
D0% or C100%	End of charge	0.00	0.09 ± 0.01
D15%	Discharged for 6 h	0.15	0.31 ± 0.02
D33%	Discharged for 13.2 h	0.33	0.46 ± 0.02
D50%	Discharged for 20 h	0.50	0.64 ± 0.03
D67%	Discharged for 26.8 h	0.67	0.76 ± 0.06
D80%*	Discharged down to 2.4 V	0.80	0.87 ± 0.06
D@cycle10	Cycled 10 times in the 5-2.4 V voltage range.	0.75	0.82 ± 0.03

* the 2.4 V end voltage cutoff has been kept constant in a potentiostatic hold with a capacity cutoff of a nominal 0.8 lithium equivalent re-insertion.

Table S2. Assignments of the observed FTIR absorption bands accordingly with the available literature[1] for the intermediate LCFMP and the final LCFMP@C materials.

Vibrational mode	Assignment	LCFMP	LCFMP@C	$LiFePO_4$ reference [1]
Intramolecular phosphate group stretching modes	ν_3	1143	**1141**	1039
	ν_3	1092	**1096**	1096
	ν_3	1058	**1063**	1065
	ν_3	1041	**1043**	1046
	ν_1	1004	**1004**	964
	ν_1	948	**970**	945
Phosphate group bending modes	ν_4	646	**646**	677
	ν_4	636	**636**	636
	$\nu_{4+}\ \nu_2$	580	**582**	576
	$\nu_{4+}\ \nu_2$	555	**555**	546
	$\nu_{4+}\ \nu_2$	507	**507**	501
	$\nu_{4+}\ \nu_2$	474	**474**	468

Table S3. Assignments of the observed Raman vibrational bands accordingly with the available literature[1] for the intermediate LCFMP and the final LCFMP@C materials.

Vibrational mode	Assignment	LCFMP	LCFMP@C	$LiFePO_4$ reference [1]
Intramolecular phosphate group stretching modes	ν_3	1075	**1069**	1071
	ν_3	1000	**999**	999
	ν_1	948 (sharp)	**951 (sharp)**	953 (sharp)
Phosphate group bending modes	ν_4	649	**653**	657
	ν_4	632	**632**	631
	ν_4			612
	ν_4	592	**588**	595
	ν_4	568		572
	ν_2			513
	ν_2	465	**452**	499
	ν_2	447	**441**	447

Table S4. Comparison of the cell parameters calculated from the XRD patterns of the intermediate LCFMP and the final LCFMP@C materials and the available literature for similar stoichiometries and lattice. Errors on the last digit are reported in parentheses.

Stoichiometry	***a* / Å**	***b* / Å**	***c* / Å**	**V / Å^3**	**Reference**
$LiCo_{1/3}Fe_{1/3}Mn_{1/3}PO_4$	10.3616(2)	6.0251(3)	4.7309(3)	295.3(1)	LCFMP, XRD this study,
	10.3351(4)	**6.0085(2)**	**4.7250(2)**	**293.4(1)**	**LCFMP@C; synchrotron XRD this study**
	10.429	**6.063**	**4.768**	**301**	**DFT+U, this study**
	10.326	6.012	4.712	292.6	Wang et al. [2] (XRD)
	10.337	6.008	4.717	292.9	Chen et al. [3] (XRD)
	10.31	5.99	4.70	290.3	Gwon et al. [4] (XRD)
	10.43	6.07	4.76	301.4	Gwon et al. [4] (DFT+U)
	10.327	6.012	4.711	292.5	Akimoto et al. [5] (XRD)
	10.328	6.012	4.713	292.8	Zhang et al.[6] (XRD)
	10.339	6.009	4.713	292.8	Li et al. [7] (XRD)
	10.330	6.009	4.715	292.7	Li et al. [8] (XRD)
$LiMnPO_4$	10.4478(4)	6.1036(3)	4.7443(2)	302.5(1)	Kim et al. [9] (XRD)
	10.54	**6.16**	**4.78**	**310**	**DFT+U, this study**
$LiFePO_4$	10.3307(2)	6.0087(1)	4.6946(1)	291.4(1)	Kim et al. [9] (XRD)
	10.44	**6.07**	**4.74**	**300**	**DFT+U, this study**
$LiCoPO_4$	10.219(2)	5.926(2)	4.707(4)	285.0(1)	Brutti et al.[10] (XRD)
	10.28	**5.97**	**4.73**	**290**	**DFT+U, this study**

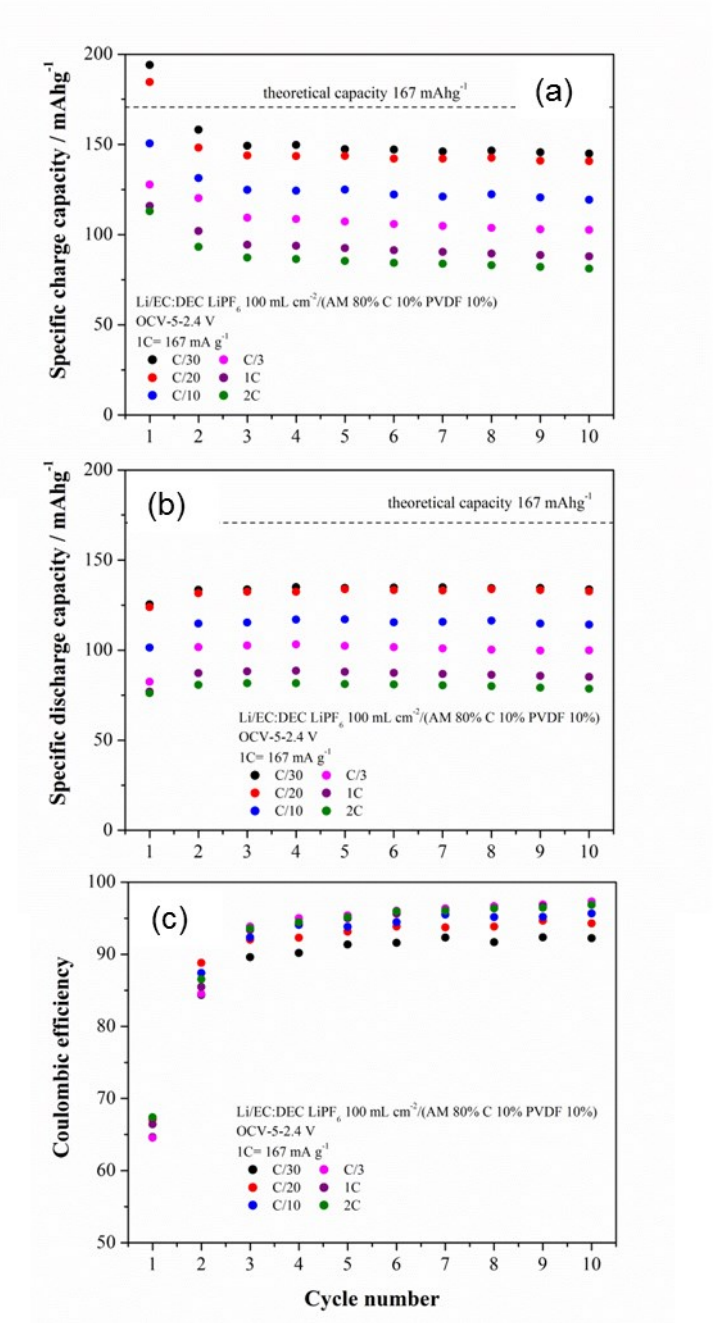

Figure S5. (a) Charge and (b) discharge specific capacity for the LCFMP@C electrodes at various current rates and (c) the corresponding Coulombic efficiencies. The specific capacity are normalized by the mass of the active material in the electrode, also including the ~7% of the carbon coating.

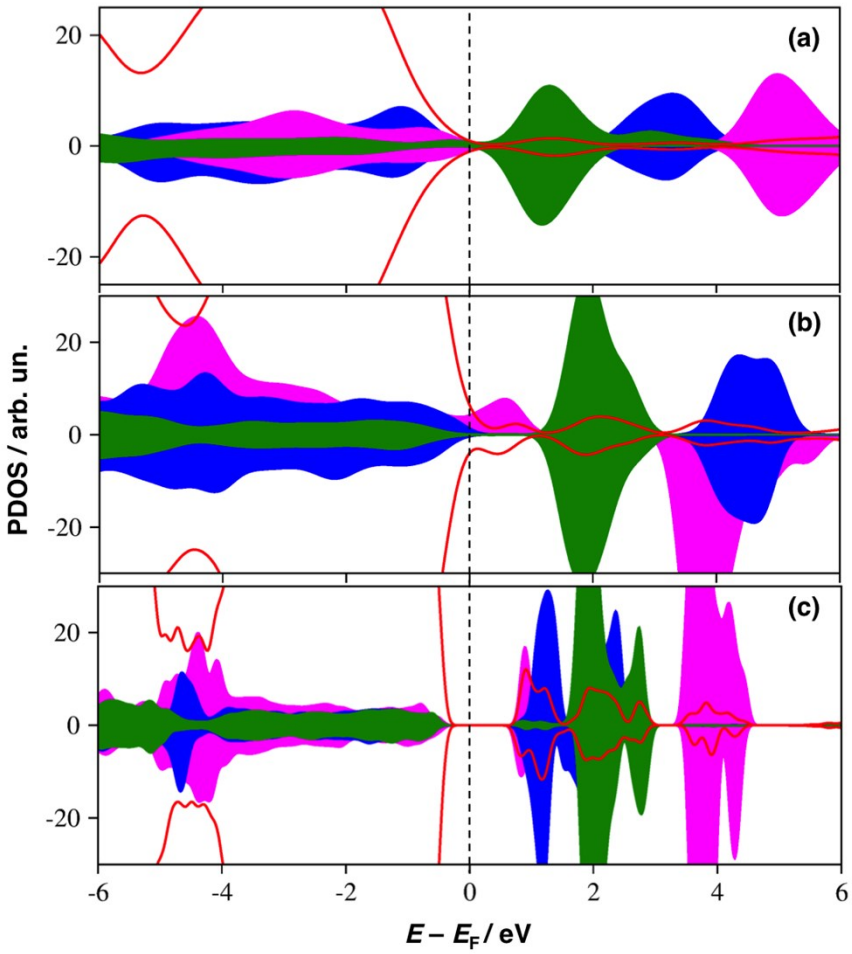

Figure S6. DFT+U computed Spin- angular-momentum and atom-projected density of states (PDOS) for LCFMP showing a sequential emptying of the electronic states after (a) 33%, (b) 66% and (c) 100% de-lithiation: E_F refers to the Fermi Energy; color legend: Co 3d (solid blue), Fe 3d (solid green), Mn 3d (solid magenta), O 2p (red line).

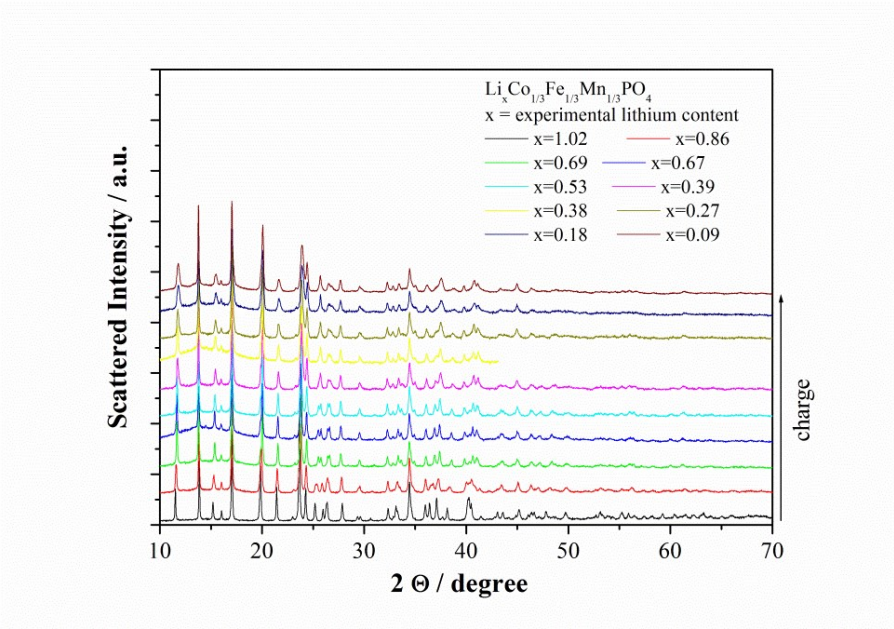

Figure S7. Evolution of the XRD patterns recorded on post mortem samples recuperated from lithium cells at various stages of charge

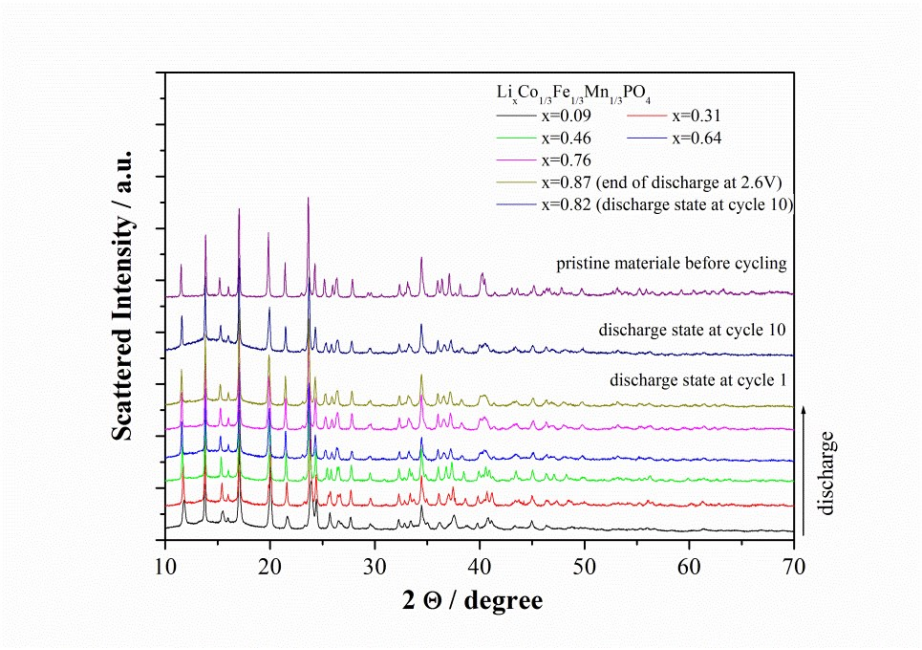

Figure S8. Evolution of the XRD patterns recorded on post mortem samples recuperated from lithium cells at various stages of discharge

Table S9. Summary of the Rietveld Refinement results for the C15% sample (R_{wp} =5.91% G.o.f. = 1.06). Errors on the last digit of the optimized atomic positions (cell axes fractions) are reported in parentheses. The Debye-Waller factors have an error of ±0.1. Experimental stoichiometry: $Li_{0.86\pm0.05}Co_{0.32\pm0.02}Mn_{0.34\pm0.02}Fe_{0.34\pm0.02}PO_4$.

Cell parameters	Atoms	Wyckoff position	Atomic coordinates x , y , z	Debye-Waller factors / A^2	Occupancies
a=10.2692±0.0003 b=5.9813±0.0002 c=4.7443±0.0002	Li Co	4°	0 , 0 , 0	0.3	0.82 0.04
	Co Fe Mn Li	4c	0.780(2) , ¼ , 0.525(2)	0.3	0.28 0.34 0.34 0.04
	P O_1 O_2 O_3	4c 4c 4c 8d	0.595(1) , ¼ , 0.082(1) 0.603(1) , ¼ , 0.759(1) 0.957(1) , ¼ , 0.293(1) 0.167(2) , 0.043(2) , 0.280(2)	0.6 0.6 0.6 0.6	1.0 1.0 1.0 1.0

Table S10. Summary of the Rietveld Refinement results for the C33% sample (R_{wp} =4.56% G.o.f. = 1.58). Errors on the last digit of the optimized atomic positions (cell axes fractions) are reported in parentheses. The Debye-Waller factors have an error of ±0.2. Experimental stoichiometry: $Li_{0.69\pm0.04}Co_{0.32\pm0.02}Mn_{0.34\pm0.02}Fe_{0.34\pm0.02}PO_4$

Cell parameters	Atoms	Wyckoff position	Atomic coordinates x , y , z	Debye-Waller factors / A^2	Occupancies
a=10.1993±0.0004 b=5.9572±0.0002 c=4.7659±0.0002	Li Co	4°	0 , 0 , 0	0.6	0.65 0.04
	Co Fe Mn Li	4c	0.779(2) , ¼ , 0.529(2)	0.6	0.28 0.34 0.34 0.04
	P O_1 O_2 O_3	4c 4c 4c 8d	0.596(1) , ¼ , 0.087(1) 0.609(1) , ¼ , 0.765(1) 0.948(1) , ¼ , 0.316(1) 0.166(2) , 0.044(2) , 0.276(2)	1.4 1.4 1.4 1.4	1.0 1.0 1.0 1.0

Table S11. Summary of the Rietveld Refinement results for the C36% sample (R_{wp} =4.53% G.o.f. = 1.49). Errors on the last digit of the optimized atomic positions (cell axes fractions) are reported in parentheses. E The Debye-Waller factors have an error of ±0.2. Experimental stoichiometry: $Li_{0.67\pm0.03}Co_{0.32\pm0.02}Mn_{0.34\pm0.02}Fe_{0.34\pm0.02}PO_4$

Cell parameters	Atoms	Wyckoff position	Atomic coordinates x , y , z	Debye-Waller factors / A^2	Occupancies
a=10.2013±0.0002 b=5.9585±0.0001 c=4.7643±0.0001	Li Co	4°	0 , 0 , 0	0.7	0.63 0.04
	Co Fe Mn Li	4c	0.779(2) , ¼ , 0.529(2)	0.7	0.28 0.34 0.34 0.04
	P O_1 O_2 O_3	4c 4c 4c 8d	0.596(1) , ¼ , 0.087(1) 0.607(1) , ¼ , 0.768(1) 0.949(1) , ¼ , 0.309(1) 0.164(2) , 0.042(2) , 0.275(2)	1.4 1.4 1.4 1.4	1.0 1.0 1.0 1.0

Table S12. Summary of the Rietveld Refinement results for the C50% sample (R_{wp} =4.53% G.o.f. = 1.49). Errors on the last digit of the optimized atomic positions (cell axes fractions) are reported in parentheses. The Debye-Waller factors have an error of ±0.2. Experimental stoichiometry: $Li_{0.53\pm0.05}Co_{0.32\pm0.02}Mn_{0.34\pm0.02}Fe_{0.34\pm0.02}PO_4$

Cell parameters	Atoms	Wyckoff position	Atomic coordinates x , y , z	Debye-Waller factors / A^2	Occupancies
a=10.1843±0.0002 b=5.9529±0.0002 c=4.7676±0.0001	Li Co	4°	0 , 0 , 0	0.6	0.48 0.05
	Co Fe Mn Li	4c	0.778(2) , ¼ , 0.529(2)	0.6	0.27 0.34 0.34 0.05
	P O_1 O_2 O_3	4c 4c 4c 8d	0.595(1) , ¼ , 0.087(1) 0.610(1) , ¼ , 0.764(1) 0.950(1) , ¼ , 0.305(1) 0.166(2) , 0.041(2) , 0.274(2)	1.2 1.2 1.2 1.2	1.0 1.0 1.0 1.0

Table S13. Summary of the Rietveld Refinement results for the C67% sample (R_{wp} =5.76% G.o.f. = 1.10). Errors on the last digit of the optimized atomic positions (cell axes fractions) are reported in parentheses. The Debye-Waller factors have an error of ±0.2. Experimental stoichiometry: $Li_{0.39\pm0.02}Co_{0.32\pm0.02}Mn_{0.34\pm0.02}Fe_{0.34\pm0.02}PO_4$

Cell parameters	Atoms	Wyckoff position	Atomic coordinates x , y , z	Debye-Waller factors / A^2	Occupancies
a=10.1427±0.0004 b=5.9452±0.0002 c=4.7743±0.0003	Li Co	4°	0 , 0 , 0	0.8	0.32 0.07
	Co Fe Mn Li	4c	0.778(2) , ¼ , 0.534(2)	0.8	0.25 0.34 0.34 0.07
	P O_1 O_2 O_3	4c 4c 4c 8d	0.594(1) , ¼ , 0.088(1) 0.615(1) , ¼ , 0.768(1) 0.958(1) , ¼ , 0.307(1) 0.170(2) , 0.040(2) , 0.266(2)	1.2 1.2 1.2 1.2	1.0 1.0 1.0 1.0

Table S14. Summary of the Rietveld Refinement results for the C70% sample (R_{wp} =5.05% G.o.f. = 1.48). Errors on the last digit of the optimized atomic positions (cell axes fractions) are reported in parentheses. The Debye-Waller factors have an error of ±0.2. Experimental stoichiometry: $Li_{0.38\pm0.02}Co_{0.32\pm0.02}Mn_{0.34\pm0.02}Fe_{0.34\pm0.02}PO_4$

Cell parameters	Atoms	Wyckoff position	Atomic coordinates x , y , z	Debye-Waller factors / A^2	Occupancies
a=10.1450±0.0005 b=5.9469±0.0003 c=4.7708±0.0003	Li Co	4°	0 , 0 , 0	0.6	0.32 0.06
	Co Fe Mn Li	4c	0.778(2) , ¼ , 0.531(2)	0.6	0.26 0.34 0.34 0.06
	P O_1 O_2 O_3	4c 4c 4c 8d	0.596(1) , ¼ , 0.086(1) 0.611(1) , ¼ , 0.763(1) 0.956(1) , ¼ , 0.311(1) 0.171(2) , 0.038(2) , 0.274(2)	1.2 1.2 1.2 1.2	1.0 1.0 1.0 1.0

Table S15. Summary of the Rietveld Refinement results for the C80% sample (R_{wp} =6.06% G.o.f. = 1.06). Errors on the last digit of the optimized atomic positions (cell axes fractions) are reported in parentheses. The Debye-Waller factors have an error of ±0.2. Experimental stoichiometry: $Li_{0.27\pm0.02}Co_{0.32\pm0.02}Mn_{0.34\pm0.02}Fe_{0.34\pm0.02}PO_4$

Cell parameters	Atoms	Wyckoff position	Atomic coordinates x , y , z	Debye-Waller factors / A^2	Occupancies
a=10.1235±0.0005 b=5.9418±0.0004 c=4.7756±0.0004	Li Co	4°	0 , 0 , 0	1.0	0.20 0.07
	Co Fe Mn Li	4c	0.778(2) , ¼ , 0.537(2)	1.0	0.25 0.34 0.34 0.07
	P O_1 O_2 O_3	4c 4c 4c 8d	0.598(1) , ¼ , 0.086(1) 0.620(1) , ¼ , 0.760(1) 0.971(1) , ¼ , 0.305(1) 0.177(2) , 0.032(2) , 0.261(2)	1.2 1.2 1.2 1.2	1.0 1.0 1.0 1.0

Table S16. Summary of the Rietveld Refinement results for the C90% sample (R_{wp} =5.92% G.o.f. = 1.13). Errors on the last digit of the optimized atomic positions (cell axes fractions) are reported in parentheses. The Debye-Waller factors have an error of ±0.2. Experimental stoichiometry: $Li_{0.18\pm0.02}Co_{0.32\pm0.02}Mn_{0.34\pm0.02}Fe_{0.34\pm0.02}PO_4$

Cell parameters	Atoms	Wyckoff position	Atomic coordinates x , y , z	Debye-Waller factors / A^2	Occupancies
a=10.1021±0.0004 b=5.9399±0.0003 c=4.7787±0.0003	Li Co	4°	0 , 0 , 0	1.9	0.11 0.07
	Co Fe Mn Li	4c	0.778(2) , ¼ , 0.538(2)	1.9	0.25 0.34 0.34 0.07
	P O_1 O_2 O_3	4c 4c 4c 8d	0.596(1) , ¼ , 0.089(1) 0.623(1) , ¼ , 0.763(1) 0.967(1) , ¼ , 0.313(1) 0.177(2) , 0.034(2) , 0.255(2)	1.9 1.9 1.9 1.9	1.0 1.0 1.0 1.0

Table S17. Summary of the Rietveld Refinement results for the fully charged (de-lithiated) C100% (or D0%) sample (R_{wp} =4.90% G.o.f. = 1.01). Errors on the last digit of the optimized atomic positions (cell axes fractions) are reported in parentheses. The Debye-Waller factors have an error of ±0.2. Experimental stoichiometry: $Li_{0.09\pm0.01}Co_{0.32\pm0.02}Mn_{0.34\pm0.02}Fe_{0.34\pm0.02}PO_4$

Cell parameters	Atoms	Wyckoff position	Atomic coordinates x , y , z	Debye-Waller factors / A^2	Occupancies
a=10.0734±0.0002 b=5.9282±0.0002 c=4.7706±0.0002	Li Co	4°	0 , 0 , 0	1.9	0.01 0.08
	Co Fe Mn Li	4c	0.777(2) , ¼ , 0.538(2)	1.9	0.24 0.34 0.34 0.08
	P	4c	0.598(1) , ¼ , 0.086(1)	1.6	1.0
	O_1	4c	0.622(1) , ¼ , 0.759(1)	1.6	1.0
	O_2	4c	0.967(1) , ¼ , 0.310(1)	1.6	1.0
	O_3	8d	0.177(2) , 0.034(2) , 0.264(2)	1.6	1.0

Table S18. Summary of the Rietveld Refinement results for the D15% sample (R_{wp} =4.96% G.o.f. = 1.56). Errors on the last digit of the optimized atomic positions (cell axes fractions) are reported in parentheses. The Debye-Waller factors have an error of ±0.2. Experimental stoichiometry: $Li_{0.31\pm0.02}Co_{0.32\pm0.02}Mn_{0.34\pm0.02}Fe_{0.34\pm0.02}PO_4$

Cell parameters	Atoms	Wyckoff position	Atomic coordinates x , y , z	Debye-Waller factors / A^2	Occupancies
a=10.1646±0.0004 b=5.9493±0.0002 c=4.7690±0.0002	Li Co	4°	0 , 0 , 0	0.5	0.24 0.07
	Co Fe Mn Li	4c	0.779(2) , ¼ , 0.530(2)	0.5	0.25 0.34 0.34 0.07
	P O_1 O_2 O_3	4c 4c 4c 8d	0.596(1) , ¼ , 0.087(1) 0.610(1) , ¼ , 0.760(1) 0.950(1) , ¼ , 0.303(1) 0.169(2) , 0.039(2) , 0.274(2)	1.7 1.7 1.7 1.7	1.0 1.0 1.0 1.0

Table S19. Summary of the Rietveld Refinement results for the D33% sample (R_{wp} =4.72% G.o.f. = 1.65). Errors on the last digit of the optimized atomic positions (cell axes fractions) are reported in parentheses. The Debye-Waller factors have an error of ±0.2. Experimental stoichiometry: $Li_{0.46\pm0.02}Co_{0.32\pm0.02}Mn_{0.34\pm0.02}Fe_{0.34\pm0.02}PO_4$

Cell parameters	Atoms	Wyckoff position	Atomic coordinates x , y , z	Debye-Waller factors / A^2	Occupancies
a=10.2278±0.0002 b=5.9658±0.0002 c=4.7562±0.0001	Li Co	4°	0 , 0 , 0	0.5	0.40 0.06
	Co Fe Mn Li	4c	0.779(2) , ¼ , 0.527(2)	0.5	0.26 0.34 0.34 0.06
	P O_1 O_2 O_3	4c 4c 4c 8d	0.595(1) , ¼ , 0.086(1) 0.606(1) , ¼ , 0.761(1) 0.949(1) , ¼ , 0.300(1) 0.167(2) , 0.040(2) , 0.275(2)	1.7 1.7 1.7 1.7	1.0 1.0 1.0 1.0

Table S20. Summary of the Rietveld Refinement results for the D50% sample (R_{wp} =5.38% G.o.f. = 1.44). Errors on the last digit of the optimized atomic positions (cell axes fractions) are reported in parentheses. The Debye-Waller factors have an error of ±0.2. Experimental stoichiometry: $Li_{0.64\pm0.03}Co_{0.32\pm0.02}Mn_{0.34\pm0.02}Fe_{0.34\pm0.02}PO_4$

Cell parameters	Atoms	Wyckoff position	Atomic coordinates x , y , z	Debye-Waller factors / A^2	Occupancies
a=10.2798±0.0004 b=5.9827±0.0002 c=4.7400±0.0002	Li Co	4°	0 , 0 , 0	0.8	0.58 0.06
	Co Fe Mn Li	4c	0.779(2) , ¼ , 0.528(2)	0.8	0.26 0.34 0.34 0.06
	P O_1 O_2 O_3	4c 4c 4c 8d	0.593(1) , ¼ , 0.082(1) 0.609(1) , ¼ , 0.761(1) 0.947(1) , ¼ , 0.293(1) 0.164(2) , 0.044(2) , 0.275(2)	2.1 2.1 2.1 2.1	1.0 1.0 1.0 1.0

Table S21. Summary of the Rietveld Refinement results for the D67% sample (R_{wp} =4.90% G.o.f. = 1.38). Errors on the last digit of the optimized atomic positions (cell axes fractions) are reported in parentheses. The Debye-Waller factors have an error of ±0.2. Experimental stoichiometry: $Li_{0.76\pm0.06}Co_{0.32\pm0.02}Mn_{0.34\pm0.02}Fe_{0.34\pm0.02}PO_4$

Cell parameters	Atoms	Wyckoff position	Atomic coordinates x , y , z	Debye-Waller factors / A^2	Occupancies
a=10.2840±0.0004 b=5.9858±0.0003 c=4.7393±0.0002	Li Co	4°	0 , 0 , 0	0.7	0.71 0.05
	Co Fe Mn Li	4c	0.779(2) , ¼ , 0.526(2)	0.7	0.27 0.34 0.34 0.05
	P O_1 O_2 O_3	4c 4c 4c 8d	0.595(1) , ¼ , 0.084(1) 0.603(1) , ¼ , 0.761(1) 0.953(1) , ¼ , 0.295(1) 0.166(2) , 0.043(2) , 0.279(2)	1.3 1.3 1.3 1.3	1.0 1.0 1.0 1.0

Table S22. Summary of the Rietveld Refinement results for the D80% sample (R_{wp} =4.95% G.o.f. = 1.48). Errors on the last digit of the optimized atomic positions (cell axes fractions) are reported in parentheses. The Debye-Waller factors have an error of ±0.2. Experimental stoichiometry: $Li_{0.87\pm0.06}Co_{0.32\pm0.02}Mn_{0.34\pm0.02}Fe_{0.34\pm0.02}PO_4$

Cell parameters	Atoms	Wyckoff position	Atomic coordinates x , y , z	Debye-Waller factors / A^2	Occupancies
a=10.2908±0.0003 b=5.9884±0.0002 c=4.7372±0.0001	Li Co	4°	0 , 0 , 0	0.8	0.88 0.04
	Co Fe Mn Li	4c	0.779(2) , ¼ , 0.524(2)	0.8	0.28 0.34 0.34 0.04
	P O_1 O_2 O_3	4c 4c 4c 8d	0.595(1) , ¼ , 0.085(1) 0.601(1) , ¼ , 0.762(1) 0.953(1) , ¼ , 0.293(1) 0.166(2) , 0.043(2) , 0.280(2)	1.4 1.4 1.4 1.4	1.0 1.0 1.0 1.0

Table S23. Summary of the Rietveld Refinement results for the D@cycle10 sample (R_{wp} =4.34% G.o.f. = 1.74). Errors on the last digit of the optimized atomic positions (cell axes fractions) are reported in parentheses. The Debye-Waller factors have an error of ±0.2. Experimental stoichiometry: $Li_{0.82\pm0.03}Co_{0.32\pm0.02}Mn_{0.34\pm0.02}Fe_{0.34\pm0.02}PO_4$

Cell parameters	Atoms	Wyckoff position	Atomic coordinates x , y , z	Debye-Waller factors / A^2	Occupancies
a=10.2714±0.0002 b=5.9795±0.0001 c=4.7448±0.0001	Li Co	4°	0 , 0 , 0	0.4	0.77 0.05
	Co Fe Mn Li	4c	0.780(2) , ¼ , 0.526(2)	0.4	0.27 0.34 0.34 0.05
	P O_1 O_2 O_3	4c 4c 4c 8d	0.596(1) , ¼ , 0.084(1) 0.603(1) , ¼ , 0.759(1) 0.953(1) , ¼ , 0.296(1) 0.168(2) , 0.042(2) , 0.277(2)	1.5 1.5 1.5 1.5	1.0 1.0 1.0 1.0

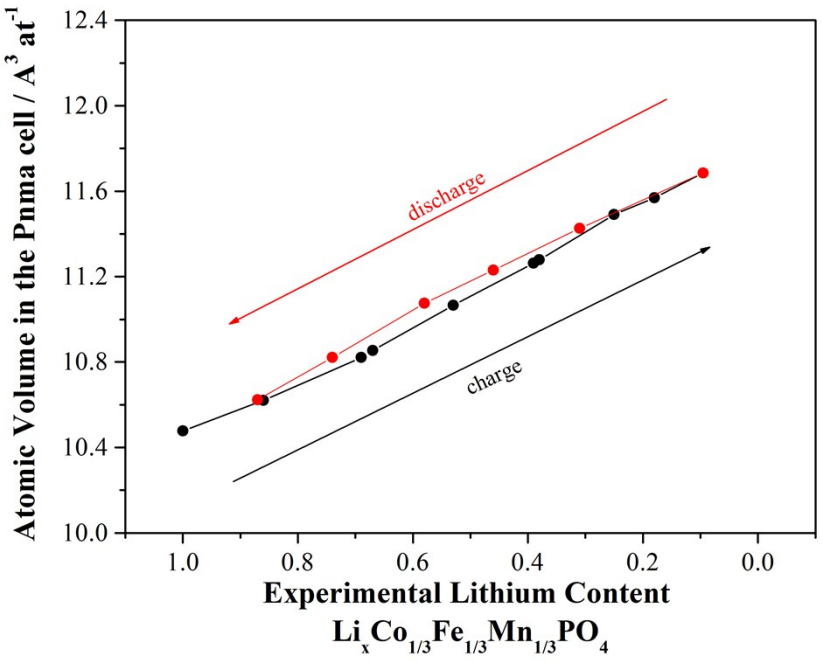

Figure S24. Evolution of the atomic volume in the Pnma orthorhombic cell upon electrochemical lithium extraction/insertion by Rietveld Refinement of the synchrotron XRD.

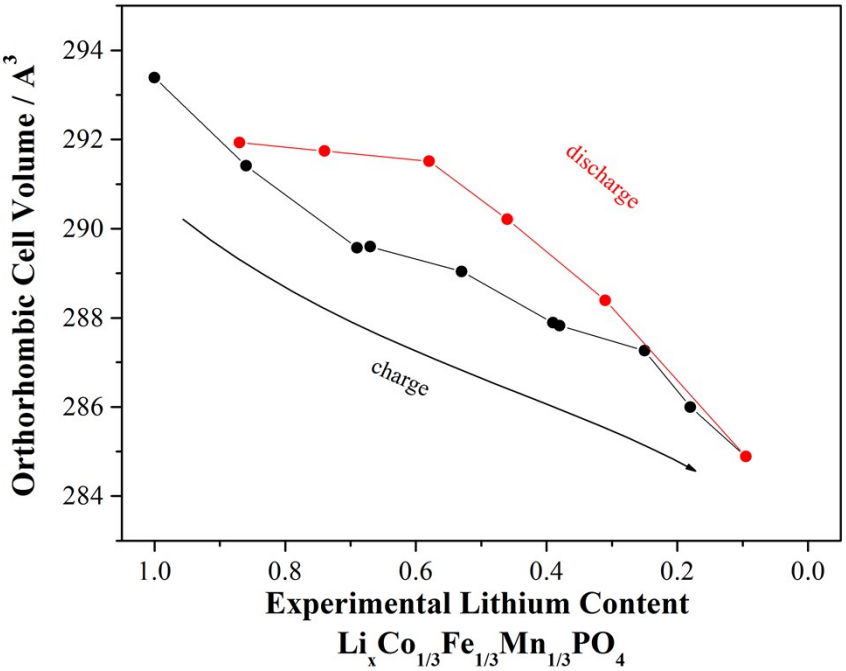

Figure S25. Evolution of Pnma orthorhombic cell volume upon electrochemical lithium extraction/insertion by Rietveld Refinement of the synchrotron XRD.

Supplementary note S26. Calculation of the Gibbs energy of mixing of the mixing of the lithiated/delithiated disordered lattices in respect to the fully ordered phases at various lithium content

The stoichiometries of the mixing reactions of the four disordered olivine lattices are:

$1/3\ LiCoPO_4 + 1/3\ LiFePO_4 + 1/3\ LiMnPO_4 \rightarrow LiCo_{⅓}Fe_{⅓}Mn_{⅓}PO_4$ R1

$1/3\ LiCoPO_4 + 1/3\ FePO_4 + 1/3\ LiMnPO_4 \rightarrow Li_{⅔}Co_{⅓}Fe_{⅓}Mn_{⅓}PO_4$ R2

$1/3\ LiCoPO_4 + 1/3\ FePO_4 + 1/3\ MnPO_4 \rightarrow Li_{⅓}Co_{⅓}Fe_{⅓}Mn_{⅓}PO_4$ R4

$1/3\ CoPO_4 + 1/3\ FePO_4 + 1/3\ MnPO_4 \rightarrow Co_{⅓}Fe_{⅓}Mn_{⅓}PO_4$ R5

Thus, the changes in the internal energies of the above reactions at 0K can be estimated by the following equations:

R1 $\Delta_{R1}U_{0K} = E_{tot}(LiCo_{⅓}Fe_{⅓}Mn_{⅓}PO_4) - ⅓\ E_{tot}(LiCoPO_4) - ⅓\ E_{tot}(LiFePO_4) - ⅓\ E_{tot}(LiMnPO_4)$

R2 $\Delta_{R120K} = E_{tot}(Li_{⅔}Co_{⅓}Fe_{⅓}Mn_{⅓}PO_4) - ⅓\ E_{tot}(LiCoPO_4) - ⅓\ E_{tot}(FePO_4) - ⅓\ E_{tot}(LiMnPO_4)$

R4 $\Delta_{R3}U_{0K} = E_{tot}(Li_{⅓}Co_{⅓}Fe_{⅓}Mn_{⅓}PO_4) - ⅓\ E_{tot}(LiCoPO_4) - ⅓\ E_{tot}(FePO_4) - ⅓\ E_{tot}(MnPO_4)$

R5 $\Delta_{R4}U_{0K} = E_{tot}(Co_{⅓}Fe_{⅓}Mn_{⅓}PO_4) - ⅓\ E_{tot}(CoPO_4) - ⅓\ E_{tot}(FePO_4) - ⅓\ E_{tot}(MnPO_4)$

Where E_{tot} are the total energies calculated for the various phases in their relaxed ground state structures from the DFT+U calculations. The four disordered lattices at 0K have a non-zero configurational entropy, $S°_{0K}$, that can be calculated by the following simple equations assuming an ideal entropy of mixing model.

$LiCo_{⅓}Fe_{⅓}Mn_{⅓}PO_4$ $S°_{0K} = 3{\cdot}R\ (⅓ \cdot \ln ⅓)$

$Li_{⅔}Co_{⅓}Fe_{⅓}Mn_{⅓}PO_4$ $S°_{0K} = 4{\cdot}R\ (⅓ \cdot \ln ⅓) + R\ (⅔ \cdot \ln ⅔)$

$Li_{⅓}Co_{⅓}Fe_{⅓}Mn_{⅓}PO_4$ $S°_{0K} = 4{\cdot}R\ (⅓ \cdot \ln ⅓) + R\ (⅔ \cdot \ln ⅔)$

$Co_{⅓}Fe_{⅓}Mn_{⅓}PO_4$ $S°_{0K} = 3{\cdot}R\ (⅓ \cdot \ln ⅓)$

Where R=8.13 J K^{-1} mol^{-1} is the gas constant. Being the configurational entropies of the ordered phases null at 0K the entropy change of the mixing reactions R1 to R4 at 0K are:

R1 $\Delta_{R1}S_{0K} = 3 \cdot R \left(\frac{1}{3} \cdot \ln \frac{1}{3}\right)$

R2 $\Delta_{R2}S_{0K} = 4 \cdot R \left(\frac{1}{3} \cdot \ln \frac{1}{3}\right) + R \left(\frac{2}{3} \cdot \ln \frac{2}{3}\right)$

R4 $\Delta_{R3}S_{0K} = 4 \cdot R \left(\frac{1}{3} \cdot \ln \frac{1}{3}\right) + R \left(\frac{2}{3} \cdot \ln \frac{2}{3}\right)$

R5 $\Delta_{R4}S_{0K} = 3 \cdot R \left(\frac{1}{3} \cdot \ln \frac{1}{3}\right)$

A reasonable estimate of the Gibbs energy changes of reactions R1 to R4 at room temperature can be obtained by applying the $\Delta G=\Delta H-T\Delta S$ equation under the following assumptions.

1) Negligible differences between internal energy and enthalpy changes for all reactions at 0K. This assumption is reasonable assuming a compensation effect among the zero point vibrational energies of the ordered and disordered lattices.
2) Negligible thermal effects between 0 and 298 K for all reactions. This assumption is reasonable in consideration of the compensation effect among the vibrational energies at finite temperature between ordered and disordered lattices.
3) Negligible difference between internal energy and enthalpy changes for all reactions between 0 and 298 K. This assumption is reasonable in consideration of the isostructural lattice of all the phases involved in the reactions R1 to R4 that likely implies similar bulk moduli and therefore a further compensation effect between ordered and disordered lattices.

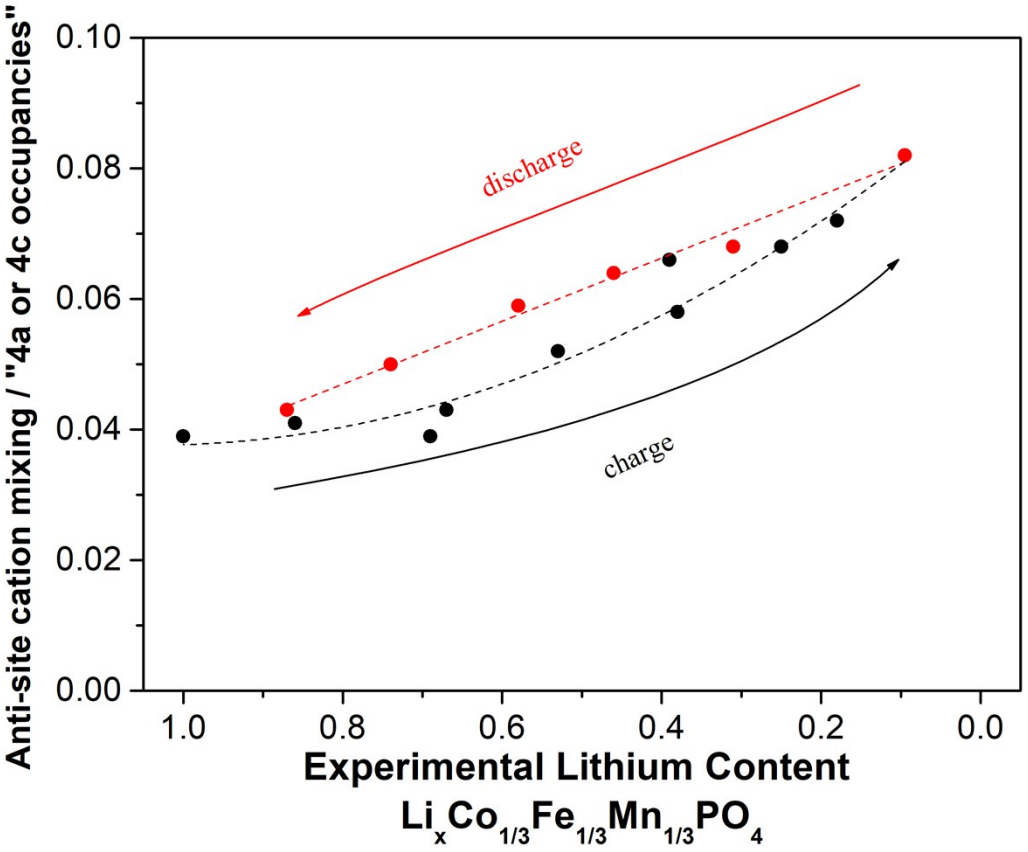

Figure S27. Evolution of 4a/4c anti-site defects upon electrochemical lithium extraction/insertion by Rietveld Refinement of the synchrotron XRD.

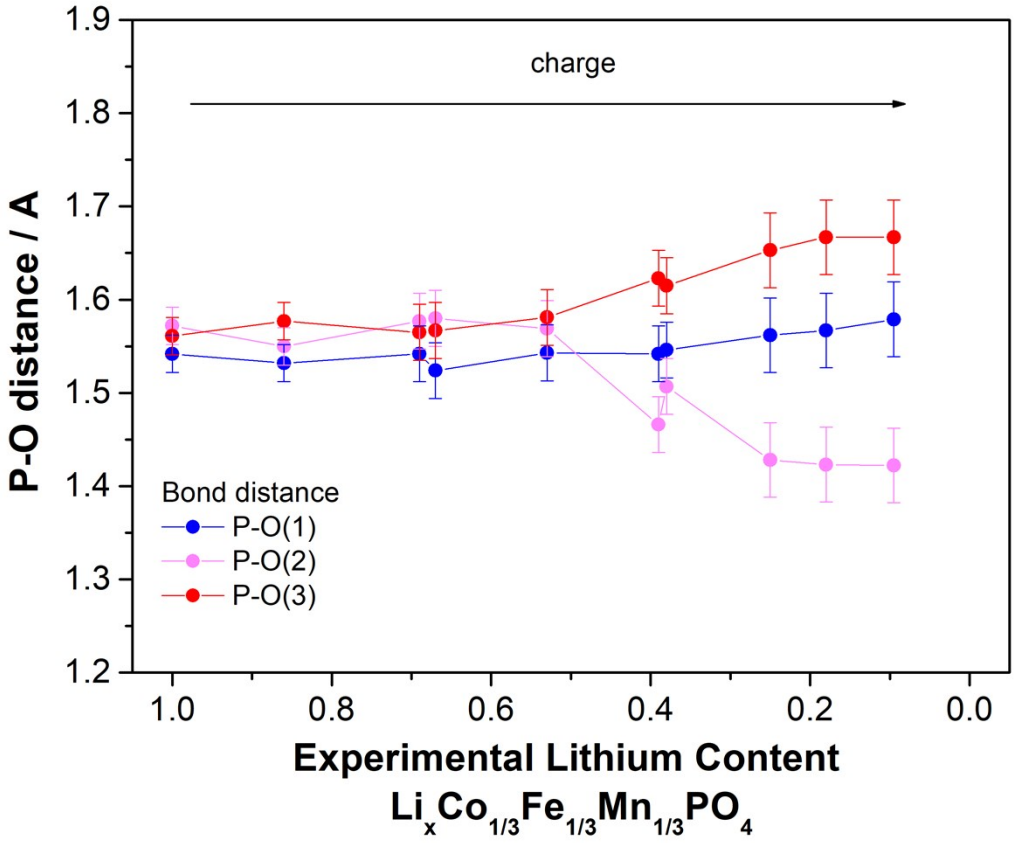

Figure S28. Experimental P-O bond distances at various lithium content in the LCFMP olivine lattice derived by the Rietveld Refinement performed on the XRD data

(1) Burba, C. M.; Frech, R. Raman and FTIR Spectroscopic Study of LixFePO4 (0 ≤ x ≤ 1). *J. Electrochem. Soc.* **2004**, *151* (7), A1032–A1038.

(2) Wang, Y.; Wang, Y.; Liu, X.; Zhu, B.; Wang, F. Solvothermal Synthesis of LiFe1/3Mn1/3Co1/3PO4 Solid Solution as Lithium Storage Cathode Materials. *RSC Adv.* **2017**, *7* (24), 14354–14359.

(3) Chen, J.; Wang, S.; Whittingham, M. S. Hydrothermal Synthesis of Cathode Materials. *J. Power Sources* **2007**, *174* (2), 442–448.

(4) Gwon, H.; Seo, D.-H.; Kim, S.-W.; Kim, J.; Kang, K. Combined First-Principle Calculations and Experimental Study on Multi-Component Olivine Cathode for Lithium Rechargeable Batteries. *Adv. Funct. Mater.* **2009**, *19* (20), 3285–3292.

(5) Akimoto, S.; Taniguchi, I. Synthesis and Characterization of LiCo1/3Mn1/3Fe1/3PO4/C Nanocomposite Cathode of Lithium Batteries with High Rate Performance. *J. Power Sources* **2013**, *242*, 627–630.

(6) Zhang, Y.; Sun, C. S.; Zhou, Z. Sol–gel Preparation and Electrochemical Performances of LiFe1/3Mn1/3Co1/3PO4/C Composites with Core–shell Nanostructure. *Electrochem. commun.* **2009**, *11* (6), 1183–1186.

(7) Li, H.; Li, Y.; Chen, L.; Jiang, H.; Wei, J.; Wang, H.; Wang, Y. Microwave Assisted Synthesis of Core–shell LiFe1/3Mn1/3Co1/3PO4/C Nanocomposite Cathode for High-Performance Lithium-Ion Batteries. *J. Alloys Compd.* **2014**, *617*, 154–159.

(8) Li, H.; Chen, Y.; Chen, L.; Jiang, H.; Wang, Y.; Wang, H.; Li, G.; Li, Y.; Yuan, Y. Improved Cycling and High Rate Performance of Core-Shell LiFe1/3Mn1/3Co1/3PO4/Carbon Nanocomposites for Lithium-Ion Batteries: Effect of the Carbon Source. *Electrochim. Acta* **2014**, *143*, 407–414.

(9) Kim, K.; Kim, J.-K. Comparison of Structural Characteristics and Electrochemical Properties of LiMPO4 (M=Fe, Mn, and Co) Olivine Compounds. *Mater. Lett.* **2016**, *176*, 244–247.

(10) Brutti, S.; Manzi, J.; De Bonis, A.; Di Lecce, D.; Vitucci, F.; Paolone, A.; Trequattrini, F.; Panero, S. Controlled Synthesis of LiCoPO4 by a Solvo-Thermal Method at 220 °c. *Mater. Lett.* **2015**, *145*, 324–327.